ELSEVIER

Microelectronics Journal 38 (2007) 235–244

Microelectronics Journal

www.elsevier.com/locate/mejo

Design of quantum filters with pre-determined reflection and transmission properties

S.A. Sofianos[a,*], G.J. Rampho[a], H. Azemtsa Donfack[a], I.E. Lagaris[a,b], H. Leeb[c]

[a]*Physics Department, University of South Africa, Pretoria 0003, South Africa*
[b]*Department of Computer Science, University of Ioannina, GR 451 10, Ioannina, Greece*
[c]*Atominstitut der Österreichischen Universitäten, Technische Universität Wien, Wiedner Hauptstraße 8-10, A-1040 Wien, Austria*

Received 28 September 2006; accepted 10 November 2006
Available online 4 January 2007

Abstract

A method based on the solution of the one-dimensional single channel inverse scattering is proposed for the design of quantum filters having specific reflection and transmission properties. The inversion procedure allows one, via modifications of a prefabricated prototype system, to reach the desired filter properties. The feasibility of the method is demonstrated on several examples, where filter properties are requested in different energy ranges. The shape and range of the corresponding potential are smooth and therefore they render themselves to applications in microelectronics, nanostractures and in quantum devices.

Keywords: Microelectronics; Nanostructures; Quantum wells; Heterostructures; Inverse scattering

1. Introduction

The inverse scattering problem on the line [1–4] was the subject of several theoretical investigations in the past and several questions concerning the inversion procedure were successfully addressed. These include the numerical solution of the Marchenko integral equation [5–8], the handling of bound states [9] and the successful solution of the coupled channel problem in the presence of thresholds and bound states [10–13].

With regard to applications, only limited use of inverse scattering techniques in one dimension has been made despite their huge prospects in a variety of fields including reflection at atomic mirrors [14], construction of semiconductor quantum devices [15] and in quantum structure development in microelectronics [16]. The corresponding lack of progress can be attributed to the fact that the solution of the inverse scattering problem presupposes the knowledge not only of the reflectivity (modulus of the reflection coefficient) but also of the corresponding phase at all incident momenta k, the measurement of which is non-trivial. For the wide field of applications only a few methods have been suggested for the complete experimental determination of the reflection coefficient. For example, in neutron reflectometry, promising procedures were proposed [17–19], but to our knowledge the experimental implementation has been limited to one rather specific setup in neutron reflectometry [20]. The missing phase information in standard scattering experiments in one-dimensional systems is similar to the well known and longstanding phase problem in diffraction analysis [21–23].

In the present work we address the question of the design of a single channel quantum filter in one dimension by *minimal* modifications of an available prefabricated system with given reflection and transmission properties. Such designs could be of extreme interest in a variety of questions related to structures on the nanometer scale such as in the so-called frustrated total reflection of cold neutrons in which the incident neutrons, due to their wave nature, suffer a total reflection in a Ni–V–Ni Fabry–Perot resonator [24]. The design of electron wave filters from inverse scattering theory is also of interest and Bessis et al. [25] illustrated this by giving specifications for the construction of a two narrow band-pass 12-layer

*Corresponding author. Tel.: +27 12 4298014; fax: +27 12 4293643.
E-mail address: sofiasa@science.unisa.ac.za (S.A. Sofianos).

0026-2692/$ - see front matter © 2006 Elsevier Ltd. All rights reserved.
doi:10.1016/j.mejo.2006.11.006

$Al_cGa_{1-c}As$ filter. However, we use the inverse scattering techniques in a slightly different way than Bessis et al. Here we are interested in the necessary modifications of a given profile to accommodate certain requirements, such as full transmission within a given energy range. The method is applied to a variety of cases and the shape and the features of the resulting quantum filters are discussed.

In Section 2 we briefly recall the inverse scattering formalism and derive the required relations for the determination of the required modifications. In Section 3 we present several numerically solved examples and investigate the essential features of the profile which lead to the filtering function. Conclusions and the outlook for further applications is given in Section 4. In the appendix we give the parametrized forms of the profiles used in the examples and some details of the Obreshkov polynomials used in a smoothing procedure.

2. Formalism

The formalism of the one-dimensional inverse scattering problem and its solution is well known and for details we refer the reader to standard text books (see e.g. [2–4]) for the basic theory and to the work of Lipperheide et al. [6] for its numerical implementation. Before entering the central question of the filter design, we briefly recall for convenience the most important aspects of inverse scattering theory.

We consider the Schrödinger equation in one dimension

$$y'' + [k^2 - V(x)]y = 0, \quad -\infty < x < +\infty, \tag{1}$$

where k is the momentum of the particle (using appropriate units k^2 is equivalent to the energy) and the real potential $V(x)$ satisfies $V(x) = 0$ for $x < 0$ and in general $V(x) \to V_s$ for $x \to +\infty$. The corresponding Jost solutions are [3,6,26]

$$f_-(k,x) = \begin{cases} [e^{-i\bar{k}x} + R_+(k)e^{+i\bar{k}x}]/T_+(k), & x \to +\infty, \\ e^{-ikx}, & x < 0, \end{cases}$$

and

$$f_+(k,x) = \begin{cases} e^{i\bar{k}x}, & x \to +\infty, \\ [e^{-ikx} + R_-(k)e^{+ikx}]/T_-(k), & x < 0, \end{cases}$$

where $\bar{k} = \sqrt{k^2 - V_s}$ is the wave number in the semi-infinite region $x \to \infty$ and the potential goes to the substrate V_s.

The input in the inverse scattering procedure is the reflection coefficient $R_-(k)$ (or $R_+(k)$) which must be known for all momenta $k \in]-\infty, +\infty[$. Since we are dealing with real potentials $V(x)$ the reflection coefficient for negative values of k is given by (see e.g. [6])

$$R_\pm(-k) = R_\pm^*(k). \tag{2}$$

In the following we consider incidence from the left and suppress the corresponding subscript (i.e. $-$).

Knowing the reflection coefficient $R(k)$ one can perform the Fourier transformation to obtain the input kernel

$$B(x) = \frac{1}{2\pi}\int_{-\infty}^{+\infty} dk e^{-ikx} R(k) \tag{3}$$

to the Marchenko integral equation [2]

$$K(x,y) = -B(x+y) - \int_{-y}^{+x} dz\, K(x,z)B(z+y) \tag{4}$$

with $x \geqslant 0$, $-x < y < x$; $B(x) = 0$ for $x < 0$. Solving (4) yields the kernel $K(x,y)$ and thus the potential

$$V(x) = 2\frac{dK(x,x)}{dx} \quad \text{for } x > 0. \tag{5}$$

Formally, the solution of the inverse scattering problem is seemingly straightforward. However, its numerical implementation is sometimes tedious because of the oscillatory behavior of the integrand in the Fourier transform. Details on the numerical treatment are given in [6]. Additional numerical difficulties might also arise in the presence of bound states. Although this problem has also been solved [9], in this work we consider profiles that do not sustain bound states.

With the tools of inverse scattering theory we are now able to tackle the problem of the design of a quantum filter which provides full transmission or reflection in the momentum interval $k \in [k_a, k_b]$. Firstly, we assume that we have a prefabricated system with well-known profile $V_0(x)$ and reflection coefficient $R(k)$. Hence, we know the input kernel $B_0(x)$ and the corresponding transformation kernel $K_0(x,y)$ for all x, y with $x > y$. Looking for the profile $V(x)$ with, for example, vanishing reflectivity, in the momentum range $k \in [k_a, k_b]$ requires the solution of the Marchenko integral (4) with the appropriate input kernel $B(x)$.

However, in the design problem considered here, we already have an existing device and we only want to modify its profile to obtain the desired filter properties i.e. we want to change the reflection coefficient, within a specific energy region $[k_a, k_b]$, from its original value $R_0(k)$ to a new one $R(k)$. It is straightforward to develop an integral equation for the required modification of the profile. Subtracting the corresponding Marchenko equations (4) for the new and the prefabricated profile leads to

$$\Delta K(x,y) = -\Delta B(x+y) - \int_{-y}^{+x} dz\, K_0(x,z)\Delta B(z+y) - \int_{-y}^{+x} dz\, \Delta K(x,z)B(z+y), \tag{6}$$

where

$$\Delta B(x) = -\frac{1}{2\pi}\int_{k_a}^{k_b} dk[\Delta R(k)e^{-ikx} + \Delta R^*(k)e^{ikx}] \tag{7}$$

accounts for the desired change of the reflection coefficient $\Delta R(k) = R_0(k) - R(k)$ in the interval $[k_a, k_b]$. The required

modification of the profile is then given by

$$\Delta V(x) = 2\frac{\mathrm{d}}{\mathrm{d}x}\Delta K(x,x) \tag{8}$$

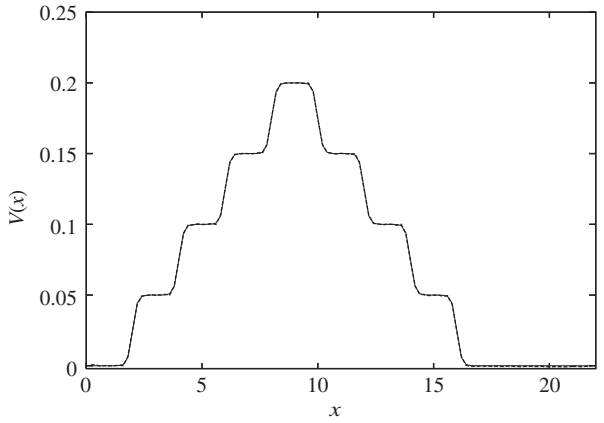

Fig. 1. The original potential and its reproduction by the Marchenko inversion procedure. The two potentials are indistinguishable.

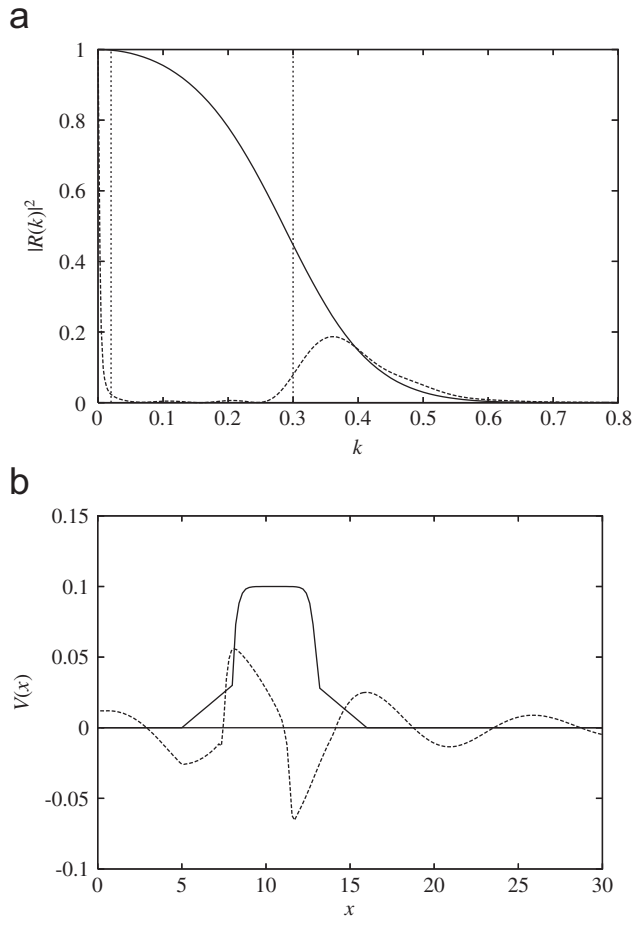

Fig. 2. (a) The input $|R(k)|^2$ (—) and the one obtained from the modified potential (- - -). The two vertical lines show the strip in which we demand $r(k) = 0$. (b) The input potential (—) and the modified one obtained by the Marchenko inversion procedure (- - -).

and thus

$$V(x) = V_0(x) + \Delta V(x). \tag{9}$$

The assumption that $R(k)$ has a specific value in the region $[k_a, k_b]$ generates discontinuities at the end points which must be healed. In the present work, we assume that the reflectivity $r(k)$ is either zero (full transmission) or one (full reflection) within a wave number region $k \in [k_a, k_b]$ and thus the continuity can be restored inside thin slices $[k_a - \delta_a, k_a]$ and $[k_b, k_b + \delta_b]$ before the inversion procedure is implemented. The healing procedure followed is different for the two cases considered.

2.1. Total reflection

The reflection coefficient is written as

$$\begin{aligned} R(k) &= a(k) + \mathrm{i}b(k) \\ &\equiv r(k)\cos\phi(k) + \mathrm{i}r(k)\sin\phi(k), \end{aligned} \tag{10}$$

where $\phi(k)$ is the phase and $\sqrt{r(k)}$ the reflectivity. In order to have total reflection we have to set $r(k) = 1$, $\forall k \in [k_a, k_b]$. The choice of phase, however, is in this case non-unique. One way to choose it, is to require that the path of the modified $\phi(k)$ in the region $[k_a, k_b]$ corresponds

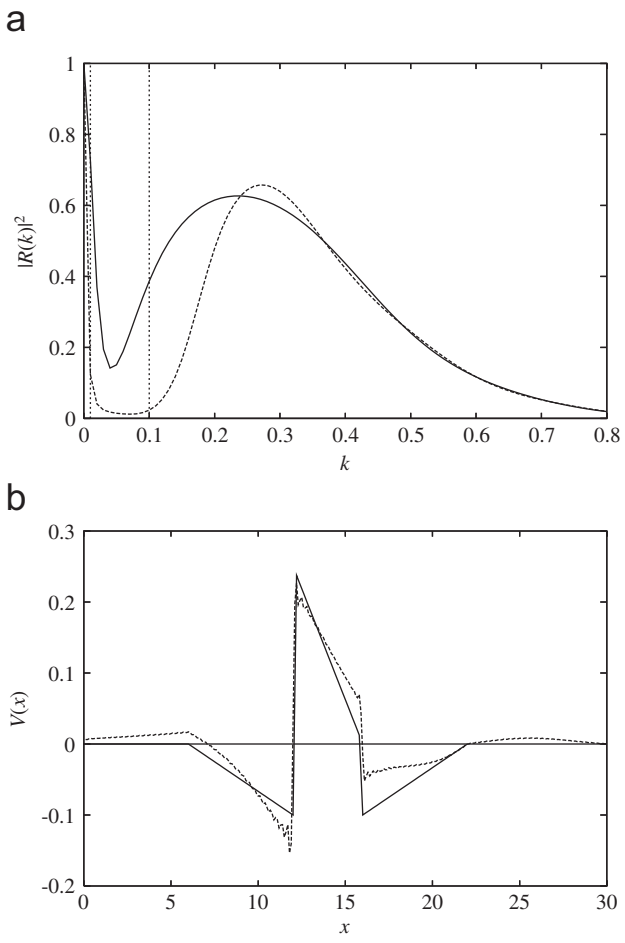

Fig. 3. Same as in Fig. 2 but with $r(k) = 0$ for $k \in (0.01, 0.1)$.

to the minimum deviation of the reflection coefficient from the original one. To achieve this we assume that ϕ depends on some adjustable parameters $\vec{v}$, $\phi(k) \equiv \phi(k, \vec{v})$, chosen so as to minimize the quantity

$$\sum_{k\in[k_a,k_b]} (a_0(k) - a(k))^2 + (b_0(k) - b(k))^2$$

i.e.

$$\sum_{k\in[k_a,k_b]} [a_0(k) - \cos(\phi(k,\vec{v}))]^2 + [b_0(k) - \sin(\phi(k,\vec{v}))]^2, \quad (11)$$

where $a_0 = \cos(\phi_0(k))$ and $b_0 = \cos(\phi_0(k))$ corresponds to the original phase and the summation is taken over all mesh k-points of the region under consideration.

The healing of the generated discontinuities is done using Obreshkov polynomials of degree three [27], to smoothly interpolate in the thin slices $k \in [k_a - \delta_a, k_a]$ and $k \in [k_b, k_b + \delta_b]$. For $a(k)$ (and similarly for $b(k)$) we have

$$a(k) = \begin{cases} a_0(k), & k \in [0, k_a - \delta_a], \\ p_3(k), & k \in [k_a - \delta_a, k_a], \\ \cos(\phi(k)), & k \in [k_a, k_b], \\ q_3(k), & k \in [k_b, k_b + \delta_b], \\ a_0(k), & k \in [k_b + \delta_b, \infty], \end{cases} \quad (12)$$

where $a_0(k)$ is the real part of the reflection coefficient obtained from the prefabricated profile, $p_3(k)$ and $q_3(k)$ are

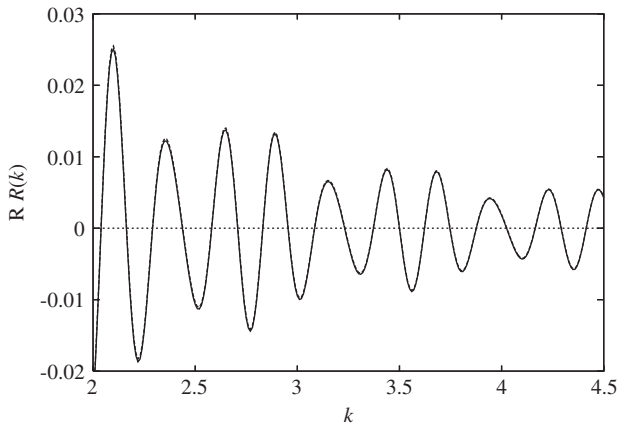

Fig. 4. The real part of $R(k)$ for the potentials shown in Fig. 3 for $k \in (2, 5)$. The two curves are indistinguishable.

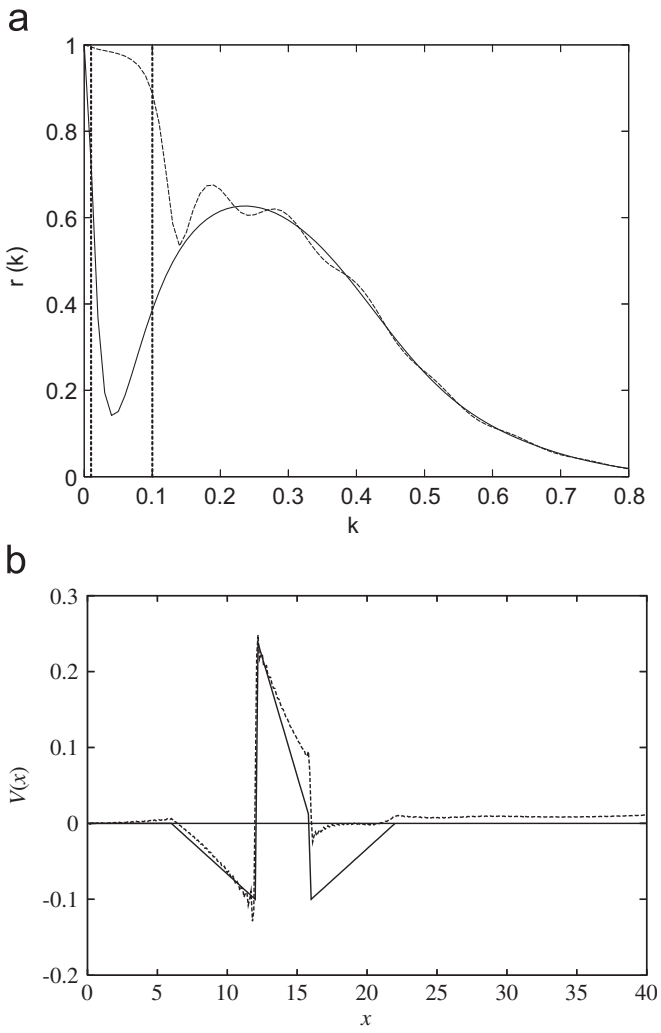

Fig. 5. Same as in Fig. 2 but with $r(k) = 1$ for $k \in (0.01, 0.1)$ and cut-off radius of $V(x)$ at $x = 40$.

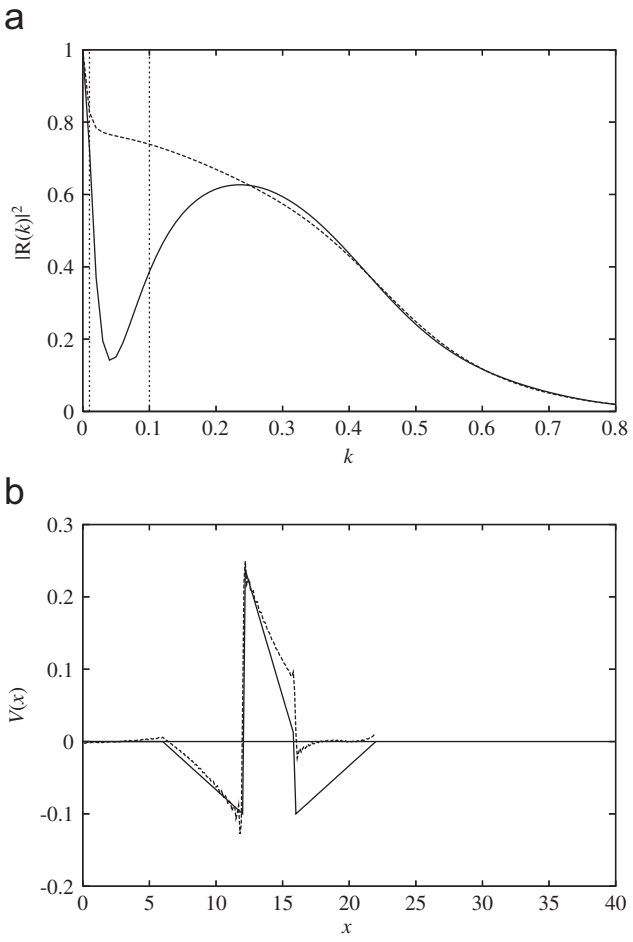

Fig. 6. Same as in Fig. 2 but with $r(k) = 1$ for $k \in (0.01, 0.1)$ and cut-off radius of $V(x)$ at $x = 22$.

Obreshkov polynomials that at both ends have prescribed function and derivative values so as to make $R(k)$ and its first derivative continuous. Using the notation of the Appendix we have

$$p_3(k) = P^{1,1}_{k_a-\delta_a,k_a}(r_0,k),$$

$$q_3(k) = P^{1,1}_{k_b,k_b+\delta_b}(r_0,k).$$

In practice, for $\phi(k,\vec{v})$ a sigmoidal perceptron [28] has been used with one hidden layer incorporating five neurons, namely,

$$\phi(k,\vec{v}) = \sum_{i=1}^{5} \frac{v_{3i-2}}{1+\exp(-v_{3i-1}k - v_{3i})}.$$

The analytic form of this function guarantees that the new phase is smooth in the region considered. The minimization of the objective function in (11) has been performed using the *Merlin* optimization environment [29].

2.2. Zero reflection

In the case $r(k) = 0$ for $k \in [k_a, k_b]$ and the choice of ϕ does not play any role. Hence for $a(k)$ (and similarly for $b(k)$) we have to take care only of the continuity at the edges,

$$a(k) = \begin{cases} a_0(k), & k \in [0, k_a - \delta_a], \\ p_3(k), & k \in [k_a - \delta_a, k_a], \\ 0, & k \in [k_a, k_b], \\ q_3(k), & k \in [k_b, k_b + \delta_b], \\ a_0(k), & k \in [k_b + \delta_b, \infty]. \end{cases} \tag{13}$$

3. Applications

Solving (1) we may calculate the reflection coefficient $R(k)$ from $k = 0$ up to a maximum value $k = K_{\max}$ for which the real and imaginary parts of $R(k)$ are of the order of $\sim 1 \times 10^{-5}$. In most examples considered here this is attained at $K_{\max} \sim 10$ (in appropriate units). Inclusion of values beyond the $K_{\max}$ has no visible effects on the reconstructed potential via inversion, and therefore they can be ignored. This can be seen in Fig. 1 where we employed, as input, a Babylonian zigurat shape potential. The original and the inverted potential are, for all practical purposes, indistinguishable. The quality of the reproduction is similar for all examples considered and from now on

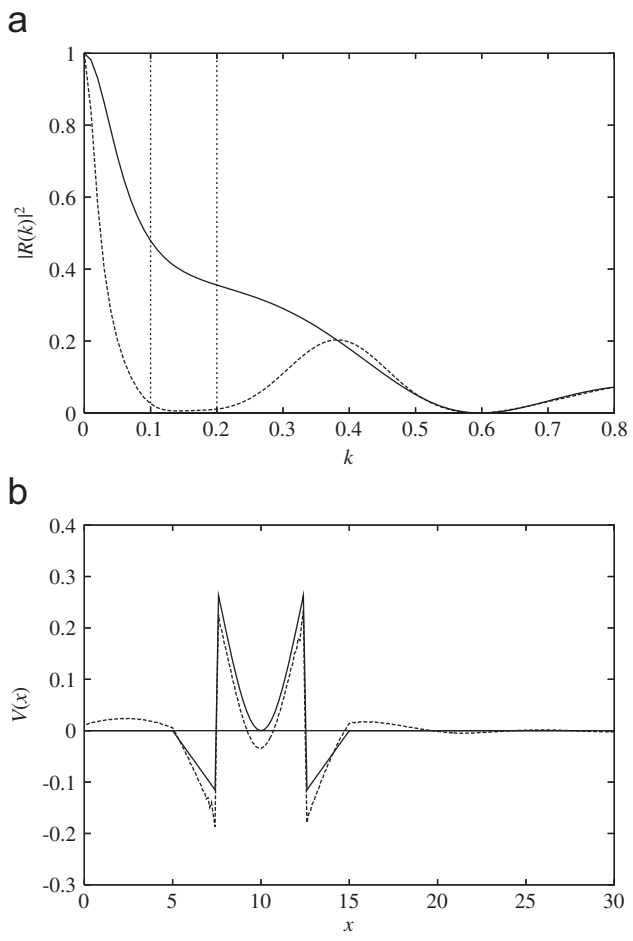

Fig. 7. Same as in Fig. 2 but with $r(k) = 0$ for $k \in (0.1, 0.2)$.

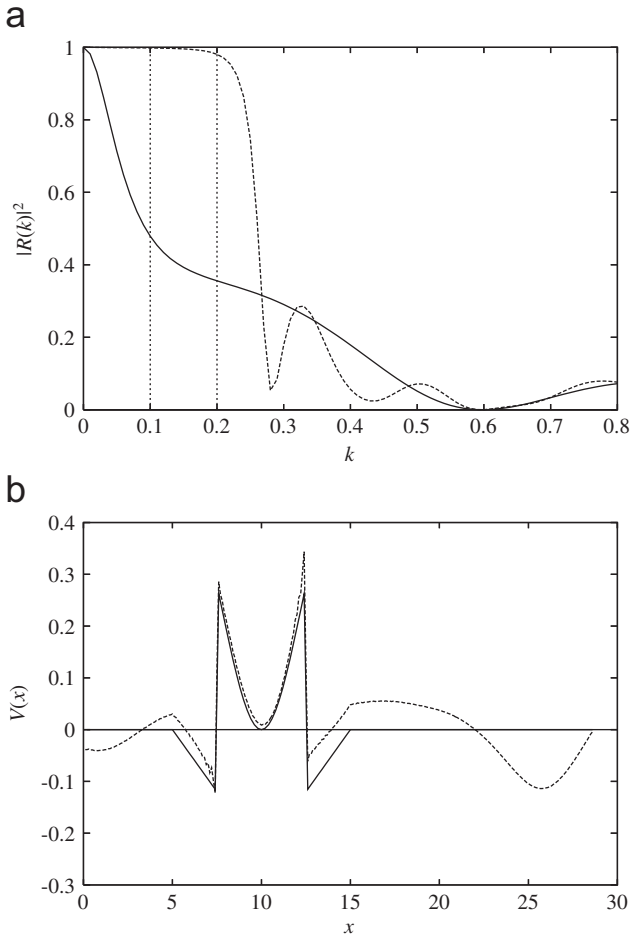

Fig. 8. Same as in Fig. 2 but with $r(k) = 1$ for $k \in (0.1, 0.2)$.

the potential obtained by inversion without modification on the reflection coefficient, will not be shown.

The first question addressed concerns the preferred form of the profile that generates a transparency at low energies which extend beyond its height. For this we consider a 'pillar' barrier of height 0.1 shown in Fig. 2(b) and impose the condition $r(k) = 0$ for $k \in (k_a, k_b) \equiv (0.02, 0.3)$. The resulting low-energy transparent potential exposes two attractive wells in either side of a triangular-type repulsion as well as a quickly diminishing oscillation beyond this range. This potential generates the reflection coefficient shown in Fig. 2(a). It is seen that within the prescribed energy region the reflection coefficient is indeed insignificant. The appearance of the triangular-type attractions and repulsions is a general trend exhibited in all cases considered with repulsive barriers. We note that the quickly diminishing small oscillations appearing beyond such a form depend on the choice of the range $k \in (k_a, k_b)$ and the way the discontinuities have been healed. It was found that the inclusion of the high energy small oscillations have insignificant effects on $r(k)$ and therefore they can be ignored. We also note that to retain the boundary condition at $k = 0$, i.e. $r(0) = 1$, k_a should never be zero.

We corroborate the above results by considering the potential shown in Fig. 3 in which triangular attractions are introduced on either side of the barrier that also has a triangular form. Prior to the modifications, the potential shape generates a reflectivity $r(k)$ which is already small and therefore with slight modifications in the shape, the resulting $r(k)$ becomes zero within the energy window $(0.01, 0.1)$. We stress here that the high energy characteristics of $R(k)$ are not affected by the modified potential. This is shown in Fig. 4 where the input and the output real part of the reflection coefficient are shown in the region $k \in (2, 5)$. Using the same potential but with the requirement that $r(k) = 1$ within the same energy range, we obtain results exhibited in Figs. 5 and 6. In the former figure, we see that the second attraction has been removed and replaced by a small substrate of the order of $k = 0.008$. By extending this substrate beyond $x \sim 50$ the reflectivity in the region $k \in (0.01, 0.1)$ becomes one. It is interesting to notice that by not including the asymptotic shape, the modifications are such that the $r(k)$ is already quite high. This is shown in Fig. 6.

Another interesting structure to consider, is the one shown in Fig. 7. By slightly shifting the edges of the

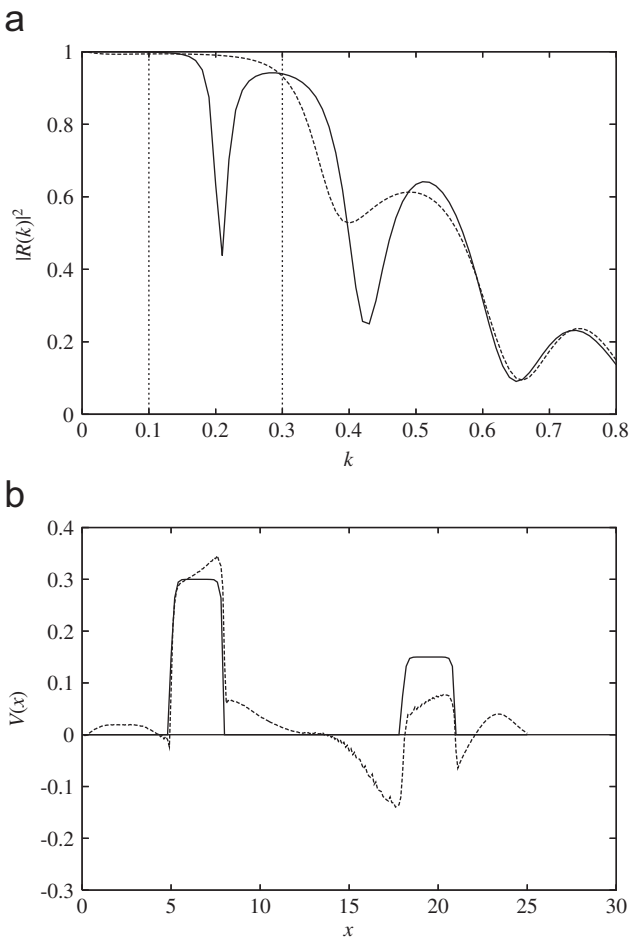

Fig. 9. Same as in Fig. 2 but with $r(k) = 1$ for $k \in (0.1, 0.3)$.

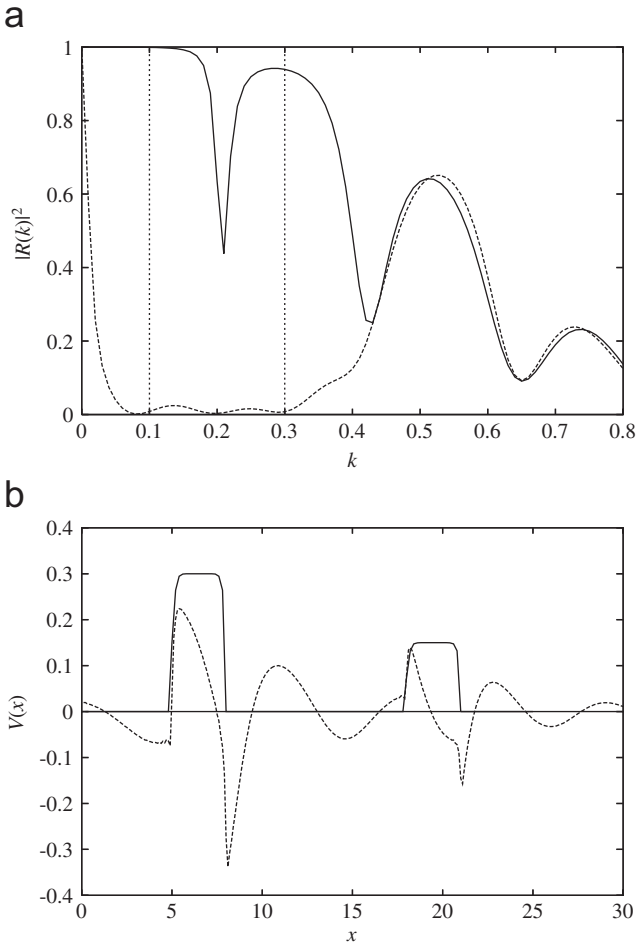

Fig. 10. Same as in Fig. 2 but with $r(k) = 0$ for $k \in (0.1, 0.3)$.

potential towards negative values a transparency is generated in the region $(0.1, 0.2)$. In contrast, the introduction of a small hump together with a small attractive components in the potential, generates full reflection in the same energy region. This is shown in Fig. 8.

Consider now a profile that consists of two barriers. By shifting the distance between the two barriers one generates either a full reflection or a relatively narrow resonance. One such double barrier profile exhibiting a resonance behavior around $k = 0.21$, which is lower that the height of the first barrier, is shown in Fig. 9. It is interesting to observe how this resonance is removed by requiring that $r(k) = 1$ up to the height of the first barrier, i.e. up to $k = 0.3$. As can be seen in Fig. 9 this is achieved by adding small repulsive parts in the first barrier region and by transforming the second barrier to have transparent characteristics shown in the previous examples. The requirement $r(k) = 0$ for $k \in (0.1, 0.3)$ provides the profile shown in Fig. 10.

As a next example, we consider again the two barrier case but with the second profile being a small attractive well as shown in Fig. 11. Although the well is quite weak and does not sustain a bound state, it, nevertheless, causes the reflectivity to be less than one in the whole energy region. The requirement that $r(k) = 0$ in $k \in (0.1, 0.25)$ can be achieved by adding an attractive and repulsive part to the potential in similar fashion to Fig. 2. In contrast the requirement $r(k) = 1$ in the same energy region, $k \in (0.1, 0.25)$, can be achieved by combining a repulsion and attraction as shown in Fig. 12.

A purely quantum mechanical case is the one in which we require that no reflection should exist for energies higher than the height of the barrier while the short k-behavior of $r(k)$ remains the same. One such example is shown in Fig. 13 for which we assume that $r(k) = 0$ for $k \geqslant 0.7$. It is seen that indeed no reflection exists at high energies. This is caused by a 'round off' of the edges of the potential, which effectively becomes of Gaussian shape, and the appearance of a small attraction beyond the profile. In general, it was found that the presence of round off edges always reduce the reflectivity at high energies.

Finally, we consider the somewhat more realistic profile similar to the one used by Mâaza et al. [24] in their studies on neutron tunneling in a Ni–Co–Ni Fabry–Perot resonator. The profile may consist of two Ni barriers and a Co well as shown in Fig. 14. The depth of the well is quite weak (-0.025) and does not sustain bound states. The whole combination generates a reflectivity which is practically one up to energies corresponding to the height

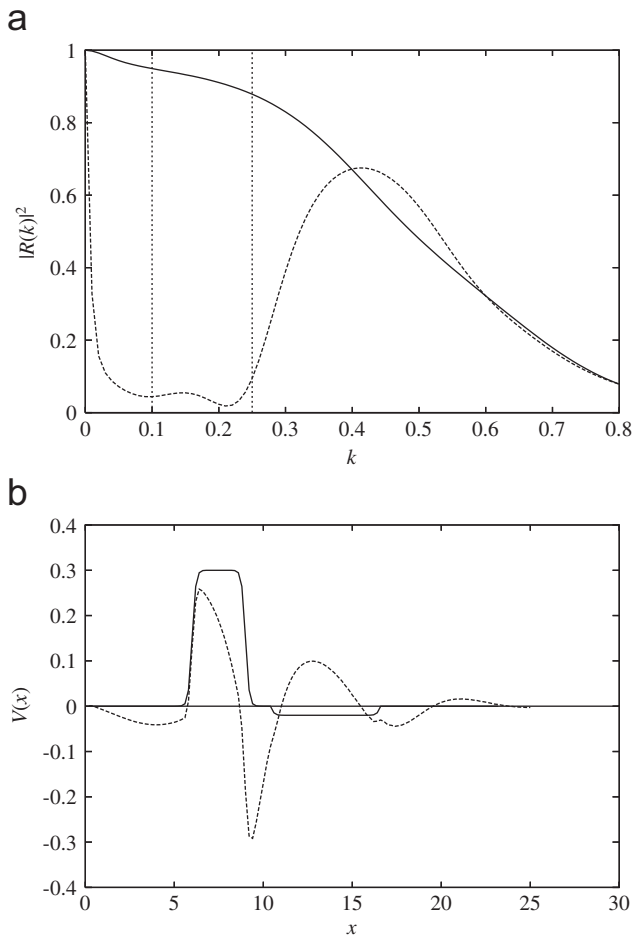

Fig. 11. Same as in Fig. 2 but with $r(k) = 0$ for $k \in (0.1, 0.25)$.

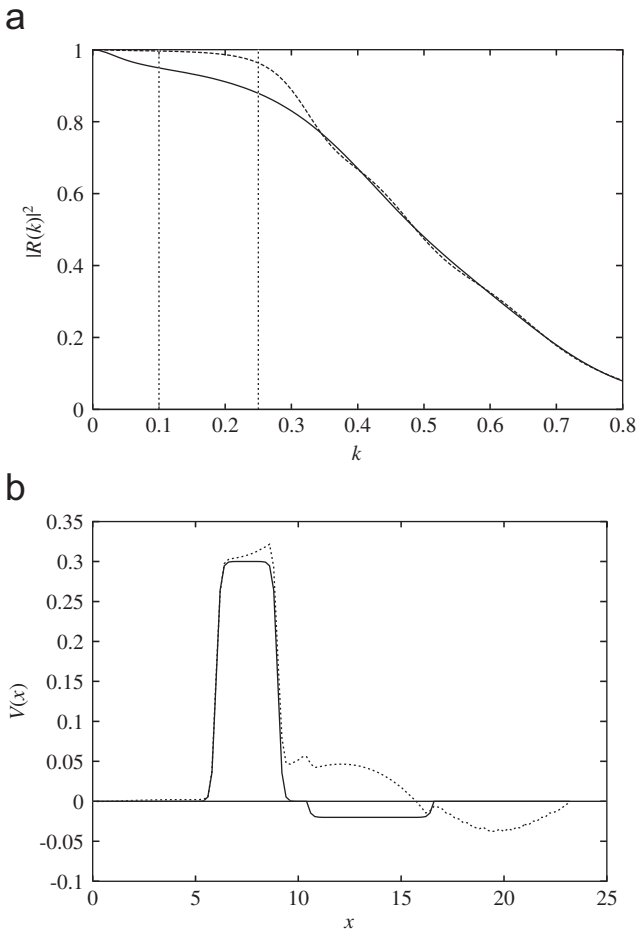

Fig. 12. Same as in Fig. 2 but with $r(k) = 1$ for $k \in (0.1, 0.25)$.

of the barriers. The necessary alterations needed to achieve $r(k) = 0$ in the region $k_b \in (0.01, 0.05)$ as well as in the wider region $k_c \in (0.01, 0.3)$ exhibit the same trends, namely the necessity to have attractive and repulsive parts in the potential of similar form to those shown in Fig. 10.

4. Summary and outlook

The one-dimensional inverse scattering problem may be used to reconstruct the potential from the knowledge of the reflection coefficient at all incident momenta. However, its application to physical problems is practically non-existent. The reason is that in experiments only the reflectivity is measured (this is the famous phase problem) and this for only a very limited range of momenta. The results up until now are frustrating and without much use in predicting the underlying potential. In the present work, we proceeded by assuming that the $R(k)$ has certain desirable reflection and transmission properties, such as a full transmission or reflection within an energy window or full transmission of all high energy waves. Then by using the one-dimensional Marchenko inversion procedure, we extracted the corresponding shape and strength of the potential which generates the required properties.

The main conclusion is that in order to achieve certain filtering properties and other desired characteristics, one may need to change only the shape of the prefabricated prototype system. The form of the modified profiles are smooth and definitely render themselves to application in microelectronics, nanostractures and other quantum devises.

The reconstructed potentials depend, of course, on the shape of the generator potential and therefore the problem is by no means exhausted with this communication whose main emphasis was to exhibit the usefulness of inverse scattering techniques in constructing and designing quantum filters. Other questions concerning various aspects of the problem can also be addressed with the present procedure. These include the construction of profiles with definite resonance structure and tunneling characteristics, the possibility of generating standing waves between two or more profiles as well as the use of real or complex potentials to control the flux of the incident waves, etc.

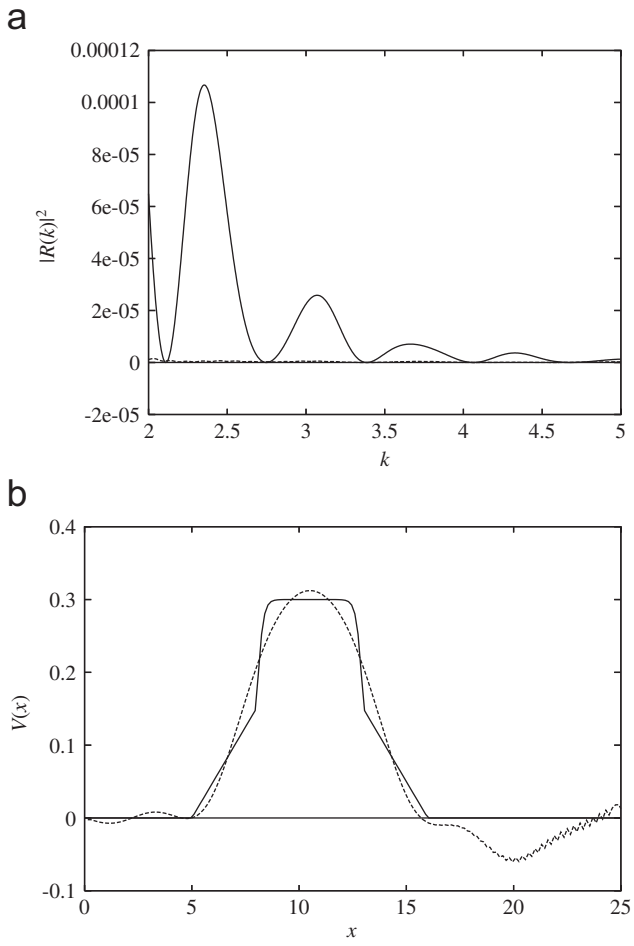

Fig. 13. Same as in Fig. 2 but with $r(k) = 0$ for $k \geqslant 0.7$. The $r(k)$ in this region, is to all practical purposes, zero.

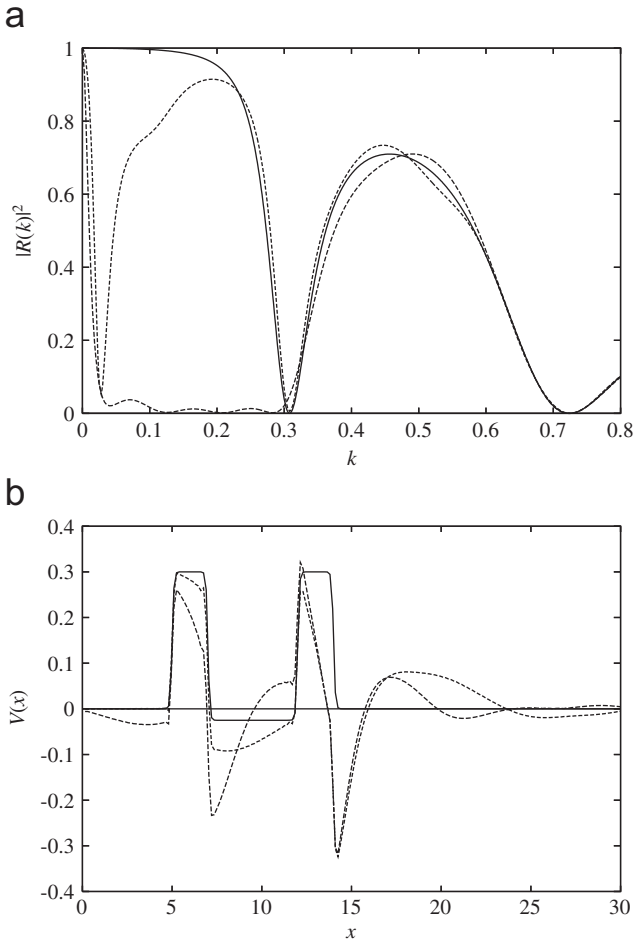

Fig. 14. A typical Ni–Co–Ni profile similar to the one used in Ref. [24] The energy ranges for which we require that $r(k) = 0$ are $k_b \in (0.01, 0.05)$ and $k_c \in (0.01, 0.3)$. The corresponding potential behavior is shown in the lower figure.

Acknowledgments

One of us (I.E.L.) wants to thank the Department of Physics of the University of South Africa for the hospitality extended to him as well as for a financial support.

Appendix A. Form of the potentials used

An N-layer barrier potential V_N can be constructed using

$$U_N(x) = \sum_{i=1}^{N}\left[\frac{V_{0i}}{1+\exp((x_i-x)/a_i)} - \frac{V_{0i}-V_s}{1+\exp((x_i+d_i-x)/a_i)}\right], \tag{A.1}$$

where x_i is the starting point for the barrier, d_i is the thickness and a_i the diffuseness parameter which for values $a_i \sim 0.01$ gives a square barrier while for higher values the edges of the barriers are trimmed and become eventually of bell-shape ($a_i \geqslant 1$). The V_s corresponds to the substrate potential.

The potential shown in Fig. 2 can be easily constructed:

$$U(x) = \begin{cases} V_0(x-x_a)/x_{L_a}, & x \in [x_a, x_b], \\ U_1(x), & x \in [x_b, x_c], \\ V_0(x_d-x)/x_{L_c}, & x \in [x_c, x_d], \\ 0 & \text{elsewhere}, \end{cases} \tag{A.2}$$

where the x_i's correspond to the starting and ending points for each branch of the potential, and x_{L_a} is the length $x_b - x_a$ and x_{L_c} the length $x_d - x_c$. The $U_1(x)$ is a one-layer potential as defined in (A.1).

Shapes of the form shown in Fig. 3 can be obtained using,

$$U(x) = \begin{cases} -V_1(x-x_a)/x_L, & x \in [x_a, x_b], \\ V_0 + V_0(x_b-x)/x_L, & x \in [x_b, x_c], \\ -V_1(x_d-x)/x_L, & \\ 0 & \text{elsewhere}. \end{cases} \tag{A.3}$$

Similarly the potential of Fig. 7 can be constructed using

$$U(x) = \begin{cases} -\dfrac{V_0}{B}\dfrac{(x-x_a)}{x_L}, & x \in [x_a, x_b], \\ V_0 - V_0\exp[-A(x-x_b-x_L)^2], & x \in [x_c, x_d], \\ -\dfrac{V_0}{B}\dfrac{(x_d-x)}{x_L}, & \\ 0 & \text{elsewhere}, \end{cases} \tag{A.4}$$

where A and B are constants and L an appropriate length (in our case $A = 0.1$, $B = 5$ and $L = 2.5$).

Appendix B. Obreshkov polynomials and related operators

Consider a continuously differentiable function $f(x)$, with $x \in [a, b]$, and a polynomial $P^{k,m}_{a,b}(f, x)$ with the properties

$$\frac{\mathrm{d}^j}{\mathrm{d}x^j}P^{k,m}_{a,b}(f,a) = \left.\frac{\mathrm{d}^j}{\mathrm{d}x^j}f(x)\right|_{x=a} \equiv f^{(j)}(a) \quad \forall\, j = 0, 1, \ldots, k,$$

$$\frac{\mathrm{d}^j}{\mathrm{d}x^j}P^{k,m}_{a,b}(f,b) = \left.\frac{\mathrm{d}^j}{\mathrm{d}x^j}f(x)\right|_{x=b} \equiv f^{(j)}(b) \quad \forall\, j = 0, 1, \ldots, m.$$

Obreshkov [27], obtained the following result for the unique polynomial of minimal degree $k + m + 1$ satisfying the above properties:

$$\begin{aligned} P^{k,m}_{a,b}(f,x) = {} & \sum_{j=0}^{k} f^{(j)}(a)\left(\frac{x-b}{a-b}\right)^{m+1}\frac{(x-a)^j}{j!} \\ & \times \sum_{i=0}^{k-j}\binom{m+i}{i}\left(\frac{x-a}{b-a}\right)^i \\ & + \sum_{j=0}^{m} f^{(j)}(b)\left(\frac{x-a}{b-a}\right)^{k+1}\frac{(x-b)^j}{j!} \\ & \times \sum_{i=0}^{m-j}\binom{k+i}{i}\left(\frac{x-b}{a-b}\right)^i. \end{aligned}$$

We may then define the 'Obreshkov operator' $L^{k,m}_{x\in[a,b]}$ applied to function $f(x)$ via the following relation:

$$L^{k,m}_{x\in[a,b]}f(x) = P^{k,m}_{a,b}(f,x). \tag{B.1}$$

We define for $x \in [a, b]$ the spline-like function

$$\begin{aligned} S^{k,m}_{a,b}(f,x) &\equiv f(x) - P^{k,m}_{a,b}(f,x) \\ &= (1 - L^{k,m}_{x\in[a,b]})f(x). \end{aligned} \tag{B.2}$$

$S^{k,m}_{a,b}(f,x)$ has the property that at $x = a$, ($x = b$) vanishes along with all its derivatives up to the kth (mth) order, and hence it behaves like a spline. We also define for $x \in [a, b]$

$$\begin{aligned} B^{k,m}_{a,b}(f,x) &\equiv f(x) - S^{k,m}_{a,b}(f,x) \\ &= [1 - (1 - L^{k,m}_{x\in[a,b]})]f(x) \\ &= L^{k,m}_{x\in[a,b]}f(x) = P^{k,m}_{a,b}(f,x). \end{aligned} \tag{B.3}$$

Note that $B^{k,m}_{a,b}(f,x)$ resembles f on the boundary, and hence it may be called a 'boundary match'. In two dimensions where the sub-domain becomes $[a_1, b_1] \otimes [a_2, b_2]$ the above definitions may generalize as

$$\begin{aligned} S(f,x_1,x_2) \equiv {} & (1 - L^{k_1,m_1}_{x_1\in[a_1,b_1]}) \\ & \times (1 - L^{k_2,m_2}_{x_2\in[a_2,b_2]})f(x_1,x_2) \end{aligned} \tag{B.4}$$

and

$$\begin{aligned} B(f,x_1,x_2) &= f(x_1,x_2) - S(f,x_1,x_2) \\ &= (L^{k_1,m_1}_{x_1\in[a_1,b_1]} + L^{k_2,m_2}_{x_2\in[a_2,b_2]} \\ &\quad - L^{k_1,m_1}_{x_1\in[a_1,b_1]}L^{k_2,m_2}_{x_2\in[a_2,b_2]})f(x_1,x_2) \end{aligned} \tag{B.5}$$

and similarly for higher dimensions. A corresponding generalization for polynomial splines in two dimensions, known as '*Spline-blended functions*' has been developed for

use in designing surfaces for technical products by Gordon [30].

References

[1] I. Kay, Commun. Pure Appl. Math. 13 (1960) 371.
[2] Z.S. Agranovich, V.A. Marchenko, The Inverse Problem of Scattering Theory, Gordon & Breach, New York, 1963.
[3] K. Chadan, P.C. Sabatier, Inverse Problems in Quantum Scattering Theory, second ed., Springer, New York, 1989.
[4] D.N. Ghosh Roy, Methods of Inverse Problems in Physics, CRC Press, Boston, 1991.
[5] R. Lipperheide, G. Reiss, H. Fiedeldey, S.A. Sofianos, H. Leeb, Physica B 221 (1992) 377.
[6] R. Lipperheide, G. Reiss, H. Leeb, H. Fiedeldey, S.A. Sofianos, Phys. Rev. B 51 (1995) 11032.
[7] R. Lipperheide, H. Fiedeldey, H. Leeb, G. Reiss, S.A. Sofianos, Physica B 213 & 214 (1995) 914.
[8] R. Lipperheide, G. Reiss, H. Leeb, S.A. Sofianos, Physica B 221 (1996) 514.
[9] M. Braun, S.A. Sofianos, R. Lipperheide, Inverse Prob. 11 (1995) L1.
[10] M. Wadati, T. Kamijo, Prog. Theor. Phys. 52 (1974) 397.
[11] F. Calogero, D. Degasperis, Nuovo Cimento B32 (1976) 201; F. Calogero, D. Degasperis, Nuovo Cimento B39 (1977) 1.
[12] S.A. Sofianos, M. Braun, R. Lipperheide, H. Leeb, Lect. Notes Phys. 488 (1997) 54.
[13] M. Braun, S.A. Sofianos, H. Leeb, Phys. Rev. A 68 (2003) 012718.
[14] B. Segev, R. Cote, M.G. Raizen, Phys. Rev. A 56 (1997) R3350.
[15] D. Bessis, G.A. Mezincescu, Microelectron. J. 30 (1999) 953.
[16] E.E. Mendez, K. von Klitzing (Eds.), Proceedings of a NATO Advanced Study Institute on Physics and Applications of Quantum Wells and Superlattices, April 21–May 1, 1987, Erice, Sicily, Italy, NATO ASI Series, vol. 170, Plenum Press, New York, 1988.
[17] C.F. Majkrzak, N.F. Berk, Physica B 221 (1996) 520.
[18] J. Kasper, H. Leeb, R. Lipperheide, Phys. Rev. Lett. 80 (1998) 2614.
[19] H. Leeb, H. Grötz, J. Kasper, R. Lipperheide, Phys. Rev. B 63 (2002) 045414 (and references therein).
[20] C.F. Majkrzak, N.F. Berk, J. Dura, S. Atija, A. Karim, J. Pedulla, R.D. Deslattes, Physica B 248 (1998) 338.
[21] J.M. Cowley, Diffraction Physics, North Holland, Amsterdam, 1975.
[22] R.E. Burge, M.A. Fiddy, A.H. Greenaway, G. Ross, Proc. R. Soc. (London) A 350 (1976) 191.
[23] M.V. Klibanov, P.E. Sacks, J. Math. Phys. 33 (1992) 3813.
[24] M. Mâaza, B. Baro, J.P. Chauvineau, A. Raynal, A. Menelle, F. Bridou, Phys. Lett. A 223 (1996) 145.
[25] D. Bessis, G. Mantica, G.A. Mezincescu, D. Vrînceanu, Europhys. Lett. 37 (1997) 151.
[26] F. Calogero, D. Degasperis, Spectral Transform and Solitons, vol. 1, North-Holland, Amsterdam, 1982.
[27] N. Obreshkov, On the mechanical quadratures, J. Bulgar. Acad. Sci. Arts LXV-8 (1942) 191.
[28] C.M. Bishop, Neural Networks for Pattern Recognition, Clarendon press, Oxford, 1995.
[29] D.G. Papageorgiou, I.N. Demetropoulos, I.E. Lagaris, Comput. Phys. Commun. 109 (1998) 227.
[30] W.J. Gordon, Spline-blended surface interpolation through curve networks, J. Math. Mech. 18 (1969) 931.